Acta Crystallographica Section F
Structural Biology and Crystallization Communications
ISSN 1744-3091

Overexpression, crystallization and preliminary X-ray crystallographic analysis of Nudix hydrolase Orf141 from *Escherichia coli* K-1

Junho Jung,[a] Yeh-Jin Ahn[b] and Lin-Woo Kang[a]*

[a]Department of Advanced Technology Fusion, Konkuk University, Hwayang-dong, Gwangjin-gu, Seoul 143-701, South Korea, and [b]Division of Life Science, College of Natural Sciences, Sangmyung University, Hongji-dong 7, Jongno-gu, Seoul 110-743, South Korea

Correspondence e-mail: lkang@konkuk.ac.kr

Received 14 July 2007
Accepted 14 August 2007

Nudix hydrolases are a family of proteins that contain the characteristic amino-acid sequence GX_5EX_7REUXEEXGU (where U is usually I, L or V), the Nudix signature sequence. They catalyze the hydrolysis of a variety of nucleoside diphosphate derivatives such as nucleoside triphosphates, nucleotide sugars, ADP-ribose, dinucleotide coenzymes, diadenosine oligophosphates and capped RNAs. Recently, three new Nudix hydrolases have been found from *Escherichia coli*; one of them is Orf141, which cleaves pyrimidine deoxynucleoside triphosphates. Orf141 was cloned directly from *E. coli* K1 strain and was overexpressed in *E. coli* without any extra residues. Orf141 crystals were successfully obtained using polyethylene glycol 1500 as a precipitant at 285 K. X-ray diffraction data were collected to 3.1 Å resolution using synchrotron radiation. The crystal is a member of the rhombohedral space group $H32$, with unit-cell parameters $a = b = 182.2$, $c = 62.3$ Å, $\alpha = 90$, $\beta = 90$, $\gamma = 120^\circ$ (hexagonal setting). Two or three monomers are likely to be present in the asymmetric unit, with corresponding V_M values of 2.92 and 1.95 Å^3 Da^{-1} and solvent contents of 57.9 and 36.9%, respectively.

1. Introduction

The Nudix superfamily (InterPro IPR000086; Pfam PF00293) is found in all classes of organism from virus to human and hydrolyses diverse compounds including nucleoside triphosphates, nucleotide sugars, ADP-ribose, dinucleotide coenzymes, diadenosine oligophosphates and capped RNAs (McLennan, 2006). All substrates have a common structure consisting of a **nu**cleoside **di**phosphate linked to another moiety, ***X*** (Bessman *et al.*, 1996). After the Nudix signature, GX_5EX_7REUXEEXGU (where U is usually Ile, Leu or Val), was found in MutT of *Escherichia coli* and MutX of *Streptococcus pneumoniae*, Nudix hydrolases have been systematically searched for in genome data banks. MutT, the first Nudix hydrolase, efficiently cleaves the mutagenic oxidized nucleotide 8-oxo-dGTP into 8-oxo-dGMP and PP_i, thus decreasing the rate of spontaneous mutation. Disruption of *mutT* causes an ~1000-fold rise in the frequency of spontanous mutation (Yanofsky *et al.*, 1966). Both MutT and MutX have antimutator activities and the function of Nudix hydrolases was originally proposed to be a housecleaning role eliminating toxic oxidized nucleotides, but soon various compounds other than mutagenic nucleotides were identified as substrates of Nudix hydrolases and their functions were expanded to controlling the levels of metabolic intermediates and signalling compounds (McLennan, 2006). The roles played by Nudix hydrolases now include RNA processing, Ca^{2+}-channel gating, activation of alcohol dehydrogenase and regulation of extracellular signal-regulated kinase (ERK) signalling (Chu *et al.*, 2004; Dunckley & Parker, 1999; Kloosterman *et al.*, 2002; Kuhn & Luckhoff, 2004).

Recently, a new Nudix hydrolase which prefers pyrimidine deoxynucleoside triphosphates as substrates was found in *E. coli* (Xu *et al.*, 2006). MutT prefers 8-oxo-dGTP and its K_m for 8-oxo-dGTP is 10^3–10^4 times lower than that for dGTP (Ito *et al.*, 2005). NudG

```
          |←  Nudix Signature  →|
MutT      GGKIEMGETPEQAVVRELQEEVGITPQ        dGTPase
Orf141    GGGVEPGERIEEALRREIREELGEQLL        dTTPase
Orf17     TGSVEEGETAPQAAMREVKEEVTIDVV        dATPase
Orf176    QGGINPGESAEQAMYRELFEEVGLSRK        Ap4Ase
Orf257    AGFVEVGETLEQAVAREVMEESGIKVK        NADH Ppase
Orf209    AGMIEEGESVEDVARREAIEEAGLIVK        ADP-ribase
```

Figure 1
The conserved Nudix signature sequences of several Nudix hydrolases from *E. coli* are aligned and their major substrates are shown. The Nudix signature residues are shown in bold.

favours 5-Me-dCTP and 5-oxo-CTP over dCTP and CTP (O'Handley *et al.*, 2001). A *nudG*$^{-}$ strain has increased spontaneous and H_2O_2-induced mutation frequency. NudB hydrolyses both 8-oxo-dATP and 8-oxo-dADP and has a similar activity for unoxidized dATP and dADP (O'Handley *et al.*, 1996). NudB was shown to be essential for aerobic growth in rich media (Gerdes *et al.*, 2003). The preference of Orf141 for dTTP completes the set of enzymes in *E. coli* for the four canonical deoxynucleoside triphosphates. Orf141 hydrolyses dTTP into dTMP and inorganic pyrophosphate according to the reaction (Xu *et al.*, 2006)

$$\mathrm{dTTP} + \mathrm{H_2O} \rightarrow \mathrm{dTMP} + \mathrm{PP_i}.$$

The previously determined crystal structures of several Nudix hydrolases show that all Nudix hydrolases have the conserved Nudix fold. The Nudix signature-sequence residues are involved in coordinating divalent metal ions such as Mg^{2+} or Mn^{2+} at the active site (Fig. 1) and other residues upstream and downstream of the Nudix signature are responsible for substrate specificity (Kang, Gabelli, Bianchet *et al.*, 2003; Kang, Gabelli, Cunningham *et al.*, 2003; Mildvan *et al.*, 2005). A novel Nudix hydrolase Orf141 from *E. coli*, which consists of 141 amino-acid residues (16.3 kDa), prefers dTTP. In order to illuminate the structural and functional features of Orf141, we expressed, purified and crystallized Orf141 and conducted a preliminary X-ray crystallographic analysis.

2. Methods and results

2.1. Cloning

The gene for Orf141, *yfaO*, was amplified *via* the polymerase chain reaction by a colony PCR of *E. coli* K1 strain. The sequences of the forward and reverse oligonucleotide primers designed from the published genome sequence were 5′-GGC CGG **CAT ATG** CGA CAA CGG ACT ATT GTA TGC C-3′ and 5′-GCC GG**G GAT CC**T TAC AGA AGA CCT TTC AAA CGT A-3′, respectively. The bases in bold designate the *Nde*I and *Bam*HI digestion sites. The amplified DNA was then inserted into the *Nde*I/*Bam*HI-digested expression vector pET-11a (Novagen).

2.2. Overexpression and purification

Orf141 was overexpressed in *E. coli* BL21 (DE3) cells. The cells were grown at 310 K to an OD_{600} of 0.6 in Luria–Bertani medium containing 50 µg ml^{-1} ampicillin. Protein expression was induced by the addition of 0.5 m*M* isopropyl *β*-D-1-thiogalactopyranoside (IPTG). Cell growth was continued at 310 K for 6 h after IPTG induction and the cells were harvested by 10 min of centrifugation at 6000 rev min^{-1} (Vision VS24-SMTi V5006A rotor) at 277 K. The cell pellet was then resuspended in ice-cold lysis buffer (50 m*M* Tris–HCl pH 8.0, 150 m*M* NaCl, 5 m*M* DTT) and homogenized using a sonicator (Sonomasher). The crude cell extract was centrifuged for 30 min at 12 000 rev min^{-1} (Vision VS24-SMTi V508A rotor) at 277 K. The expressed Orf141 in the supernatant fraction was purified by two chromatographic steps. Ion-exchange chromatography on a HiTrap Q column (Amersham Pharmacia) was followed by a Superdex 75 S prep-grade column, which had been previously equilibrated with buffer *A* (50 m*M* Tris–HCl pH 8.0, 150 m*M* NaCl, 5 m*M* DTT). The homogeneity of the purified protein was assessed by SDS–PAGE (Fig. 2). The protein solution was concentrated using a Centri-Prep (Millipore) to a final concentration of 8 mg ml^{-1} in buffer *A*.

2.3. Crystallization and X-ray data collection

Initial crystallization was conducted at 283 K using the hanging-drop vapour-diffusion method on 24-well Linbro plates. Crystallization trials were conducted using Hampton Research Crystal Screen I and II screening kits. The hanging drops consisted of 1 µl

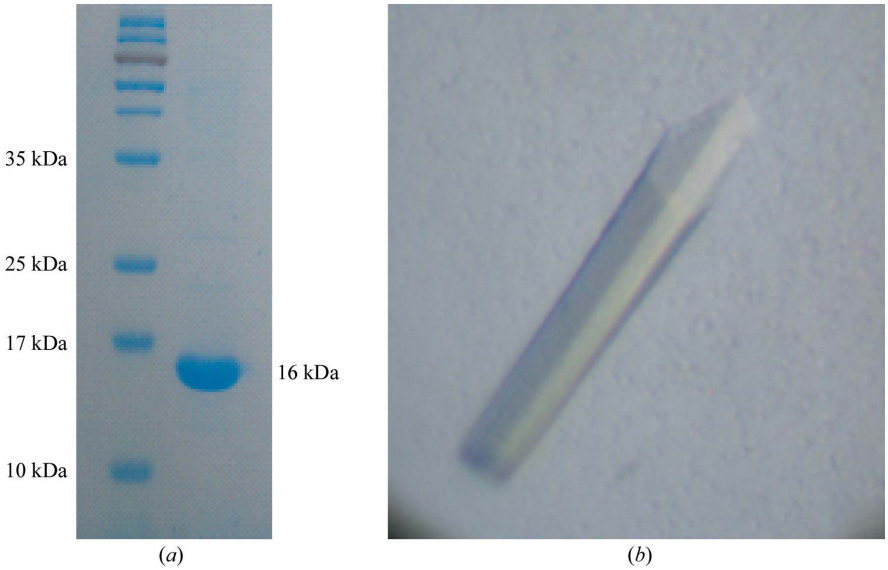

Figure 2
(*a*) Purified Orf141 is shown on a 16% SDS gel. (*b*) Crystals of Orf141 grew to dimensions of 0.5 × 0.15 × 0.15 mm in a week.

protein solution mixed with 1 µl reservoir solution. Each hanging drop was positioned over 1 ml reservoir solution. The well was sealed with a cover slip using vacuum grease. Initially, very thin needle-like crystals were observed. After optimization, rod-shaped crystals with adequate thickness were observed using a reservoir solution containing 0.1 *M* citric acid pH 5.5, 28%(*w*/*v*) PEG 1500 and 0.125 *M* sodium potassium tartrate over a period of three weeks (Fig. 2). The protein crystals were very unstable and melted away quickly on the addition of small amounts of mother liquor to the hanging drops in order to manipulate the crystals. To minimize the damage to the crystals, as soon as the wells were opened the crystals were directly mounted into a cryoloop from an existing hanging drop and flash-cooled in liquid nitrogen without any added cryoprotectant. Heavy-atom soaking was conducted by adding 0.1 µl of 5 m*M* heavy-atom solutions to the 2 µl hanging drops. The crystals were soaked overnight at 283 K for complete binding of heavy atoms. The frozen crystals were then mounted on the goniometer in a stream of cold nitrogen at 100 K. X-ray diffraction data were collected from the cooled crystals using a Bruker Proteum 300 CCD at beamline 6B at Pohang Light Source (PLS), South Korea. All native and heavy-atom-soaked crystals were oscillated by 1.0° per frame over a range of 180° at adequate wavelengths to obtain anomalous signal from each bound heavy atom. X-ray diffraction data were collected to 3.1 Å for the native and to 3.8 Å for the heavy-atom derivatives. All data were integrated and scaled using the *DENZO* and *SCALEPACK* crystallographic data-reduction routines (Otwinowski & Minor, 1997). Autoindexing was conducted with *DENZO* and the results indicated that the crystals belonged to the rhombohedral space group *H*32, with hexagonal setting unit-cell parameters $a = b = 182.2$, $c = 62.3$ Å, $\alpha = \beta = 90$, $\gamma = 120°$. Two or three monomers are likely to be present in the asymmetric unit, with corresponding calculated Matthews coefficients V_M of 2.92 and 1.95 Å^3 Da^{-1} and solvent contents of 57.9 and 36.9%, respectively (Matthews, 1968). Data-collection statistics are provided in Table 1. The self-rotation function shows that the crystallographic threefold axis is parallel to the *c* axis and the crystallographic twofold axes are perpendicular to the threefold axis with a difference of 60° (Fig. 3). The contour interval is the r.m.s. deviation of the map and the contours starts at twice the r.m.s. deviation. There are no other twofold or threefold axis peaks observed apart from crystallographic symmetry. The structure determination of Orf141 is currently under way by molecular replacement and the MIR and SIRAS experimental phasing methods and the structural details will be described in a separate paper. Our structural information regarding Orf141 will provide detailed

Table 1
Data-collection statistics.

Values in parentheses are for the outer shell.

	Native	$GdCl_3$ derivative	$SmCl_3$ derivative	Sm acetate derivative
X-ray source	Synchrotron (PAL-6B)			
Unit-cell parameters (Å)	$a = 179.3$, $b = 179.3$, $c = 61.5$	$a = 182.3$, $b = 182.3$, $c = 62.1$	$a = 183.1$, $b = 183.1$, $c = 62.0$	$a = 182.0$, $b = 182.0$, $c = 62.4$
Wavelength (Å)	0.9999	1.4797	1.5803	1.2398
Space group	*H*32	*H*32	*H*32	*H*32
Resolution (Å)	50–3.1 (3.21–3.10)	50–3.8 (3.94–3.80)	50–3.4 (3.52–3.40)	50–3.8 (3.94–3.80)
No. of unique observations	6862 (659)	3976 (369)	5574 (516)	3973 (368)
Completeness (%)	99.1 (97.9)	98.4 (94.9)	98.5 (92.8)	96.8 (92.2)
R_{sym}†	0.087 (0.282)	0.068 (0.258)	0.091 (0.397)	0.093 (0.246)
$I/\sigma(I)$	14.0 (4.8)	15.4 (7.2)	14.6 (3.1)	11.3 (5.1)

† $R_{sym} = \sum_h \sum_i |I(h)_i - \langle I(h)\rangle| / \sum_h \sum_i I(h)_i$, where $I(h)$ is the intensity of reflection h, $\sum_h$ is the sum over all reflections and $\sum_i$ is the sum over i measurements of reflection h.

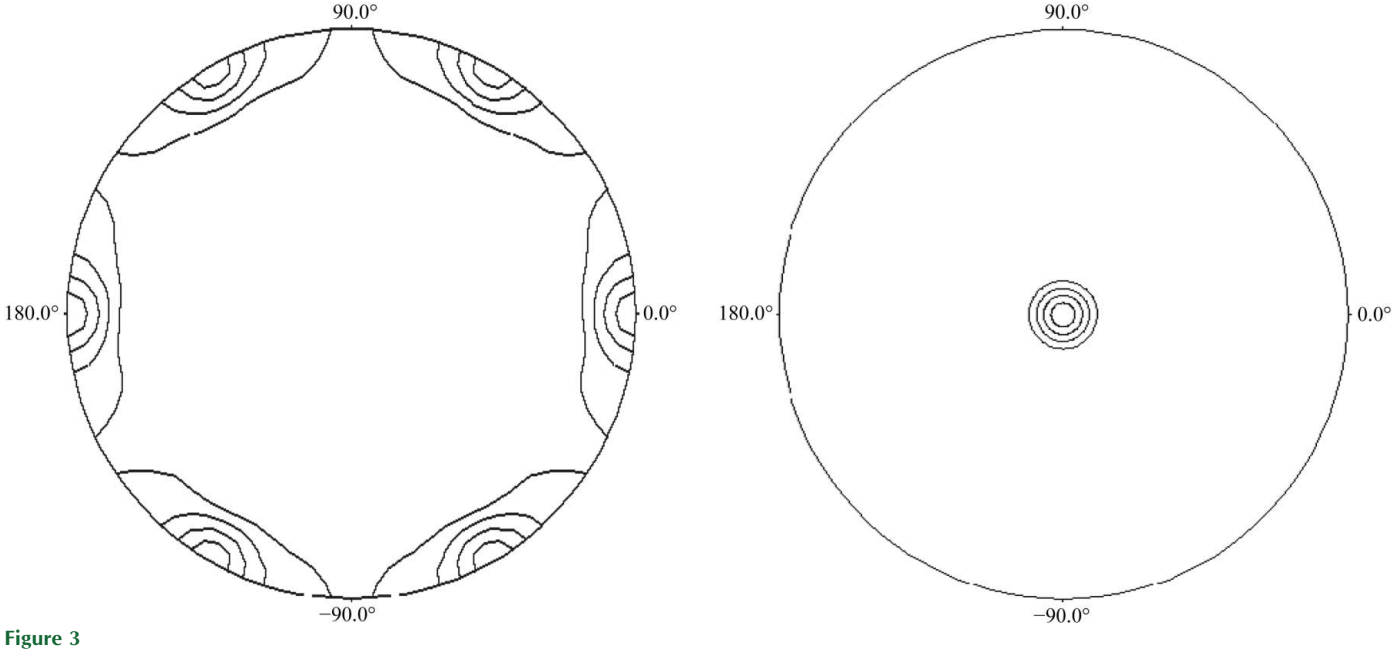

Figure 3
Self-rotation function output from *MOLREP*.

mechanisms of the recognition and hydrolysis of a specific pyrimidine nucleotide as distinct from other nucleotides.

We are grateful to Dr S. S. Cha and Dr K. J. Kim for their assistance at beamlines 6B and 6C of the Pohang Light Source (PLS), South Korea. This work was supported by a grant (Code No. 2007050103-4003) from the BioGreen 21 Program, Rural Development Administration, Republic of Korea.

References

Bessman, M. J., Frick, D. N. & O'Handley, S. F. (1996). *J. Biol. Chem.* **271**, 25059–25062.
Chu, C., Alapat, D., Wen, X., Timo, K., Burstein, D., Lisanti, M., Shears, S. & Kohtz, D. S. (2004). *Cell. Signal.* **16**, 1045–1059.
Dunckley, T. & Parker, R. (1999). *EMBO J.* **18**, 5411–5422.
Gerdes, S. Y. *et al.* (2003). *J. Bacteriol.* **185**, 5673–5684.
Ito, R., Hayakawa, H., Sekiguchi, M. & Ishibashi, T. (2005). *Biochemistry*, **44**, 6670–6674.
Kang, L. W., Gabelli, S. B., Bianchet, M. A., Xu, W. L., Bessman, M. J. & Amzel, L. M. (2003). *J. Bacteriol.* **185**, 4110–4118.
Kang, L. W., Gabelli, S. B., Cunningham, J. E., O'Handley, S. F. & Amzel, L. M. (2003). *Structure*, **11**, 1015–1023.
Kloosterman, H., Vrijbloed, J. W. & Dijkhuizen, L. (2002). *J. Biol. Chem.* **277**, 34785–34792.
Kuhn, F. J. & Luckhoff, A. (2004). *J. Biol. Chem.* **279**, 46431–46437.
McLennan, A. G. (2006). *Cell. Mol. Life Sci.* **63**, 123–143.
Matthews, B. W. (1968). *J. Mol. Biol.* **32**, 491–497.
Mildvan, A. S., Xia, Z., Azurmendi, H. F., Saraswat, V., Legler, P. M., Massiah, M. A., Gabelli, S. B., Bianchet, M. A., Kang, L. W. & Amzel, L. M. (2005). *Arch. Biochem. Biophys.* **433**, 129–143.
O'Handley, S. F., Dunn, C. A. & Bessman, M. J. (2001). *J. Biol. Chem.* **276**, 5421–5426.
O'Handley, S. F., Frick, D. N., Bullions, L. C., Mildvan, A. S. & Bessman, M. J. (1996). *J. Biol. Chem.* **271**, 24649–24654.
Otwinowski, Z. & Minor, W. (1997). *Methods Enzymol.* **277**, 307–326.
Xu, W., Dunn, C. A., O'Handley, S. F., Smith, D. L. & Bessman, M. J. (2006). *J. Biol. Chem.* **281**, 22794–22798.
Yanofsky, C., Cox, E. C. & Horn, V. (1966). *Proc. Natl Acad. Sci. USA*, **55**, 274–281.